

Imaging Experiments of Ne-like X-ray Lasers

J. C. Moreno, J. Nilsen, T. W Barbee,
L. B. Da Silva, E. Fill, Y. Li, and P. Lu

This paper was prepared for submittal to the
SPIE 1997 International Symposium on Optical
Science, Engineering, and Instrumentation
San Diego, California
July 27-August 1, 1997

June 1, 1997

This is a preprint of a paper intended for publication in a journal or proceedings. Since changes may be made before publication, this preprint is made available with the understanding that it will not be cited or reproduced without the permission of the author.



DISCLAIMER

This document was prepared as an account of work sponsored by an agency of the United States Government. Neither the United States Government nor the University of California nor any of their employees, makes any warranty, express or implied, or assumes any legal liability or responsibility for the accuracy, completeness, or usefulness of any information, apparatus, product, or process disclosed, or represents that its use would not infringe privately owned rights. Reference herein to any specific commercial product, process, or service by trade name, trademark, manufacturer, or otherwise, does not necessarily constitute or imply its endorsement, recommendation, or favoring by the United States Government or the University of California. The views and opinions of authors expressed herein do not necessarily state or reflect those of the United States Government or the University of California, and shall not be used for advertising or product endorsement purposes.

Imaging Experiments of Ne-like X-ray Lasers

Juan C. Moreno^a, Joseph Nilsen^a, Troy W. Barbee Jr.^a, Luiz B. Da Silva^a, Ernst Fill^b, Yuelin Li^c, and Peixiang Lu^b

^aLawrence Livermore National Laboratory, P. O. Box 808, Livermore, CA 94550

^bMax-Planck-Institute fur Quantenoptik, D-85748 Garching, Germany

^cUniversity of Maryland, IPST, College Park, MD 20742

ABSTRACT

We discuss high resolution two-dimensional near-field images of the neon-like nickel and germanium x-ray laser obtained using the Asterix laser at the Max-Planck-Institute and the Nova laser at Lawrence Livermore National Laboratory. Our imaging diagnostic consisted of a concave multilayer mirror that imaged the output end of the x-ray laser line onto a backside illuminated x-ray CCD detector. A 25 μm thick wire positioned at the end of the target provided a spatial fiducial. With the Asterix iodine laser, a prepulse 5.23 ns before the main pulse, was used to irradiate slab targets. A great deal of structure was observed in the near field images, particularly in the $J=0-1$ emission. We observed a large difference in the spatial dependence of the $J=0-1$ and $J=2-1$ lines of germanium, with the $J=2-1$ emission peaking farther away from the original target surface. A larger prepulse moved the peak emission farther away from the target surface. For the Nova experiments we used a series of 100 ps pulses spaced 400 ps apart to illuminate a germanium target. We obtained high resolution images of both the $J=0-1$ and $J=2-1$ lines of Ge. These measurements are compared to hydrodynamic simulations coupled with atomic kinetics and including refraction effects.

Keywords: x-ray laser, laser-plasma interaction, xuv spectroscopy

1. INTRODUCTION

Neon-like soft x-ray lasers are now being produced under a wide range of plasma conditions. Experiments have demonstrated that the $J=0-1$ line becomes the dominant line for low-Z Ne-like x-ray lasers when a prepulse is applied before the main driving laser pulse or multiple pulses are applied¹⁻⁶. Numerical simulations have indicated that using the prepulse creates a more uniform, larger scale length plasma which allows the $J=0-1$ line to propagate better. The $J=0-1$ line is predicted to appear in a higher density region than the $J=2-1$ lines since its upper level is populated primarily by collisional excitation from the ground state, while the $J=2-1$ lines on the other hand are significantly affected by recombination. Similarly when multiple pulses of equal intensity are used in the drive laser, the $J=0-1$ line can again become the dominant line compared to the $J=2-1$ line. However details of the plasma conditions and gain durations can be quite different depending on the drive pulse intensity, pulse separation, and pulse duration.

Here we investigate the effect of a prepulse and multiple pulses by analyzing experimentally measured two-dimensional spatial images of the $J=0-1$ and $J=2-1$ laser lines of Ne-like germanium and the $J=0-1$ line of Ne-like nickel from slab irradiated targets⁷⁻⁸. For the Ne-like germanium laser we present results from both a prepulse driven plasma as well as a multiple pulse driven plasma. These results are compared to hydrodynamic simulations coupled with atomic kinetics. Our measurements can not be adequately modeled without taking into account laser transport effects, including refraction. Our measurements of the spatial structure of the laser output can also be important for understanding the mode structure and coherence of soft x-ray lasers.

A typical imaging setup as used in both the Nova and Asterix experiments is shown in Fig. 1. Our imaging diagnostic consisted of a concave multilayer mirror (MoSi) which imaged the x-ray laser line onto a backside illuminated x-ray CCD detector. The CCD consisted of a 1024 by 1024 array of 24- μm pixels. The magnification was 10 for the Asterix experiments and 27.8 for the Nova experiments. Two sets of mirrors were coated, one with a peak wavelength at 19.6 nm corresponding

to the Ge J=0-1 line and the other set had a peak wavelength at 23.4 nm for the pair of Ge J=2-1 lines at 23.2 nm and 23.6 nm as well as the Ni J=0-1 line at 23.1 nm. These mirrors, which typically consisted of 20 layer pairs, have a peak reflectivity of approximately 50% and a bandpass of around 1.5 nm. For the Nova experiments an additional flat multilayer mirror was used in front of the CCD detector to relay the image and block additional background.

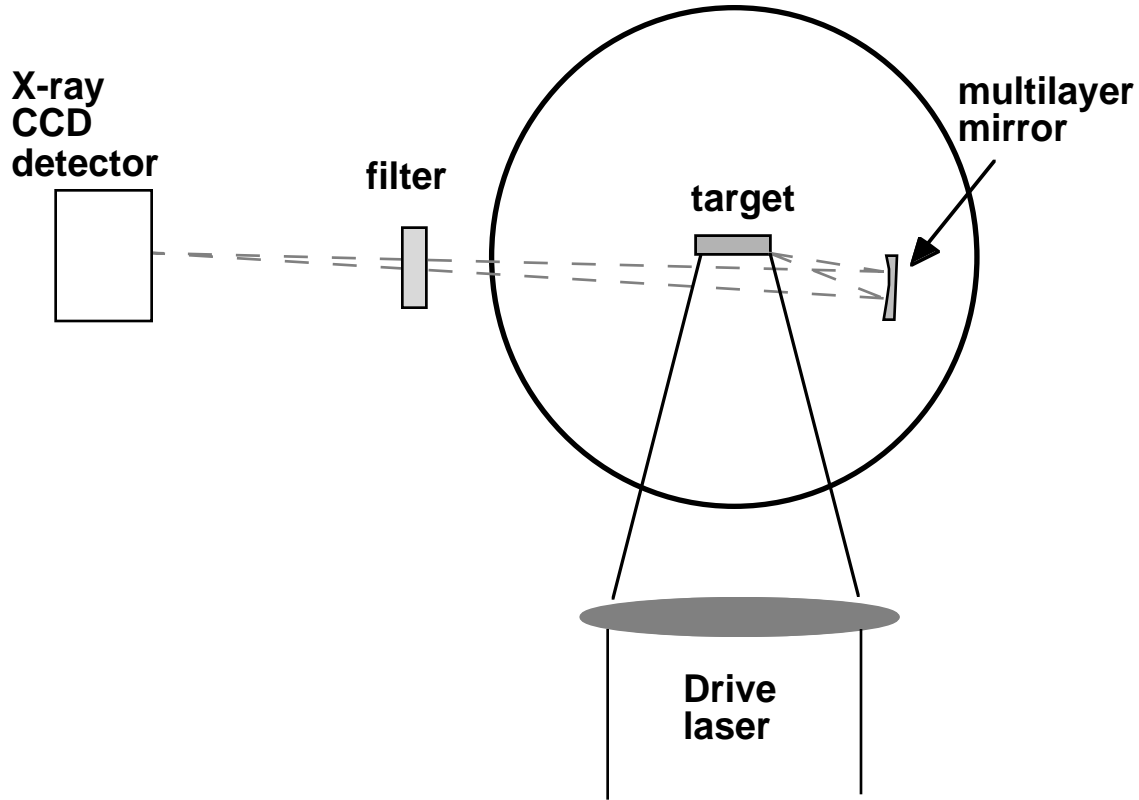


Figure 1. Schematic drawing of the experimental setup. Relative dimensions are not to scale.

The proper choice of filtering was essential to decrease the background emission and scattered light in particular since the data was time integrated. For the Asterix experiments at 19.6 nm, a 2.6 μm thick Al filter was used to eliminate short wavelength radiation below 17 nm, while a filter consisting of a 50 nm thick layer of Ti coated on a 100 nm thick Al and 188 nm thick lexan substrate was used to cutoff the long wavelength radiation above 25 nm. For the Asterix experiments at 23.4 nm, a 0.6 μm Al filter was used to eliminate the short wavelength radiation, while a 75 nm Co on 280 nm polyimide filter was used to suppress the 19.6 nm line by two orders of magnitude and reduce the long wavelength radiation.

2. ASTERIX IMAGING EXPERIMENTS

Initial imaging experiments were performed using the Asterix laser. The Asterix laser is an iodine laser with a single beam that produces as much as 600 J at 1.315 μm . Typically a 320 J, 450 ps main pulse with a prepulse (5.23 ns earlier) of varying energy was focused to a 3 cm long by 150 μm wide line focus on a slab target. To make the prepulse beam, a pair of mirrors is inserted into the beam path and a portion of the main beam is diverted and then recombined with the main beam as shown in Ref. [2]. The targets consisted of a 1 μm thick layer of germanium (or nickel) coated onto a machined flat copper substrate. A thin 25 μm wire was positioned at one end of the target at a measured distance (\sim 310 μm) off the target surface in order to provide a spatial fiducial.

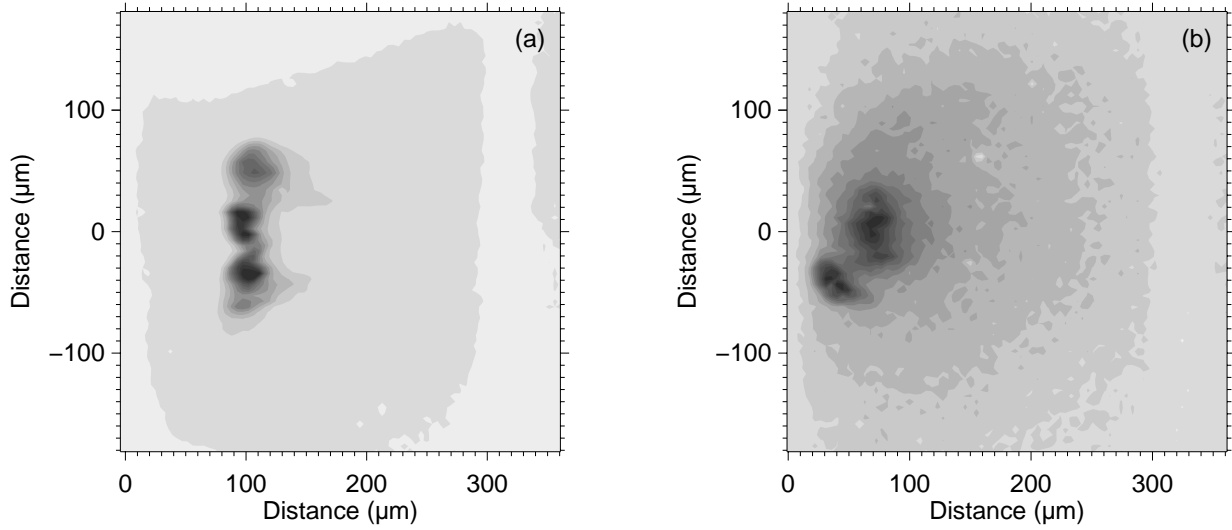


Figure 2. Two-dimensional spatial images (filled contours) of the Ne-like Ge J=0-1 line for two prepulse conditions. (a) 15% prepulse. (b) 1.65% prepulse.

Figure 2 shows spatial images of the Ge J=0-1 line at 19.6 nm obtained using two different prepulse conditions. The laser blow-off (radial) direction is the horizontal axis in the figures with zero corresponding to the original target surface. The wire fiducial is clearly evident at 310 μm from the target surface. We observe significant variations in brightness along both the radial and the transverse direction, particularly for the larger prepulse case. We believe this is partly due to the prepulse and non-uniformities in the laser focal spot which in turn produces an inhomogeneous plasma. The line focus arrangement used with the Asterix laser actually consists of six overlapping lines (due to the six section cylindrical lens array) of which two are used for the prepulse.

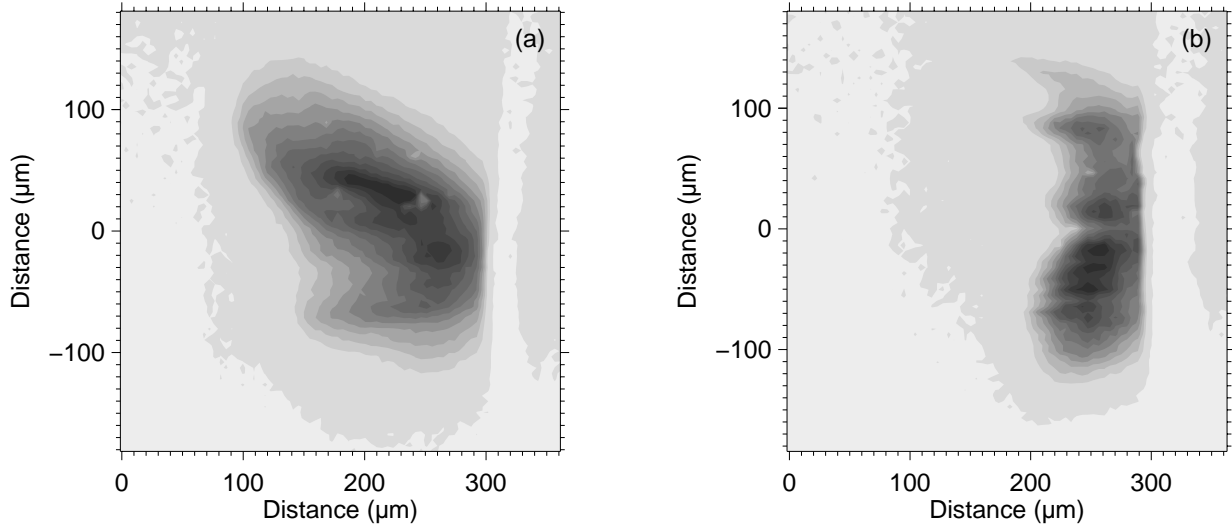


Figure 3. Two-dimensional spatial images (filled contours) of (a) Ne-like Ge J=2-1 line and (b) Ne-like Ni J=0-1 line. In both cases a 15% prepulse was used.

In Fig. 3 we show spatial images of the Ge J=2-1 lines (23.2 nm, 23.6 nm) and the Ni J=0-1 line (23.1 nm). Since these wavelengths are all within a few tenths of nm of each other, the same multilayer coating ($\lambda=23.4\text{ nm}$) was used on the mirrors

to image these lines. We observed a significant difference in the radial dependence of the x-ray laser depending on the element and the transition. The Ge $J=0-1$ line peaks at $\sim 90 \mu\text{m}$ while both the Ge $J=2-1$ lines and the Ni $J=0-1$ line peak at $\sim 250 \mu\text{m}$, although the Ni $J=0-1$ line has a somewhat sharper peak. This is consistent with numerical simulations as will be discussed later in this paper.

With a 1.65% prepulse we observed a more uniform near field emission region for all cases and in addition we observed that the peak of the emission moved radially closer to the target surface. With no prepulse our signal was not strong enough to observe these lines. Using an absolute calibration for the backside illuminated CCD detector we determined the output energy of the 19.6 nm line to be $\sim 10 \mu\text{J}$ for the 15% prepulse case and $\sim 1 \mu\text{J}$ for the 1.65% prepulse case, while the Ge $J=2-1$ energy was $\sim 10 \mu\text{J}$ for these two conditions.

3. NOVA IMAGING EXPERIMENTS

Experiments were also performed using the Nova laser at Lawrence Livermore National Laboratory. One beam of the Nova laser illuminated the germanium-coated target of length 2.52 cm with a 0.48 cm gap in the middle. The Nova laser produced a series of 100 ps full width at half maximum (FWHM) Gaussian pulses which were 400 ps apart (peak to peak). Each pulse (containing 400 J) was focused to a 120 μm wide by 3.6 cm long line focus, for a peak intensity of 110 TW/cm². The traveling wave setup was used so that the Nova beam would illuminate the target from end to end at a phase velocity equal to the speed of light⁵. These germanium targets had a 25 μm diameter wire centered 242 μm from the target surface to serve as a spatial fiducial.

Our imaging diagnostic again consisted of a concave multilayer mirror (MoSi) which imaged the x-ray laser line (with a magnification of 27.8) onto a backside illuminated x-ray CCD detector. An additional flat multilayer mirror was used in this setup. Aluminum and titanium filters were used to attenuate the signal and further eliminate background signals.

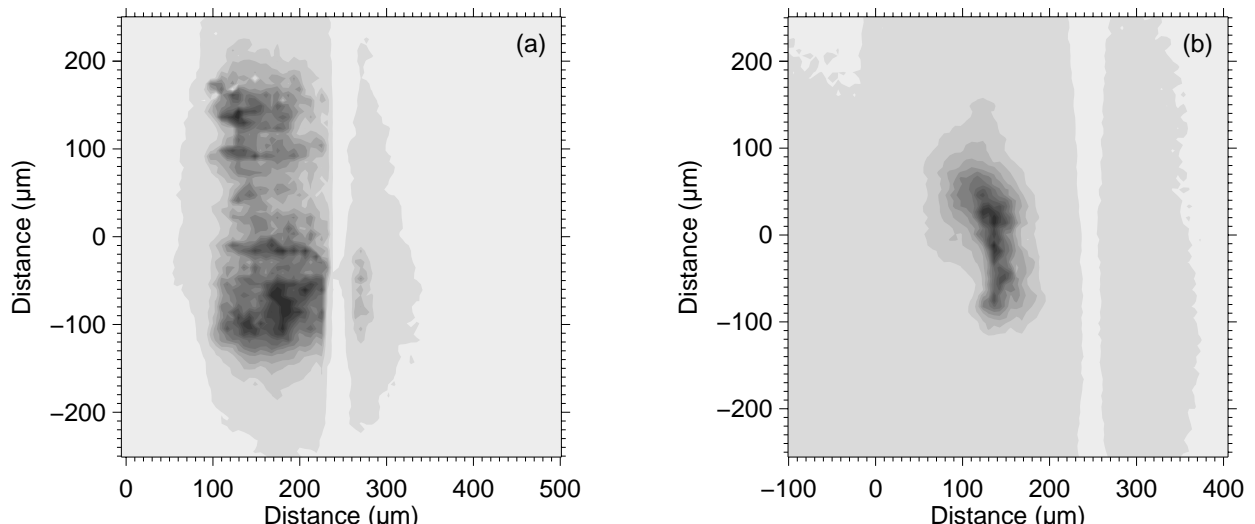


Figure 4. Two-dimensional spatial images (filled contours) of Ne-like Ge $J=0-1$ line at the output aperture of the laser. The slab targets were illuminated with either (a) three or (b) two 100-ps pulses which were 400 ps apart.

We performed a series of experiments using two or three pulses from the Nova laser. Previous experiments showed that lasing occurs during the second and third pulse and that the lasing during the third pulse is stronger by an order of magnitude. Figure 4 shows two-dimensional spatial images from the Nova experiments using two and three pulses. The experiment with two pulses used an order of magnitude less filtering in order to observe comparable signals on the CCD. For the case of two pulses, the lasing occurs closer to the surface (140 μm vs 160 μm) and has a smaller transverse extent. While the three pulse case is time integrated over the three pulses, the third pulse completely dominates the data. For the three pulse case, there is

much structure in the laser pattern and the transverse extent of the lasing region is about 300 μm , which is twice the size for the two pulse case and more than twice the transverse line focal width of the Nova laser.

4. DISCUSSION

For the Asterix experiments we observed a large change in the peak of the x-ray laser emission in the radial blow-off direction depending on the prepulse level and transition. In all cases with a larger prepulse the plasma expanded more and the peak of the x-ray laser emission moved farther from the target surface. For the Ge $J=0-1$ line the peak shifts from 70 μm to 90 μm when going from a 1.65% prepulse level to a 15% prepulse, while the Ge $J=2-1$ emission peaks are at 150 μm and 250 μm for the 1.65% prepulse and 15% prepulse cases respectively. This is due to recombination playing a much larger role in populating the $J=2-1$ upper level. In Fig. 5(a) we show calculated contour plots of gain as a function of both time and radial distance from the target for the 15% prepulse and no prepulse conditions (Asterix conditions), while Fig. 5(b) shows contour plots of the gain for the three pulse Nova experiment. We used a 1-D hydrodynamic model (LASNEX) and calculated the gain using a postprocessor (XRASER)⁹⁻¹⁰. The densities and temperatures calculated using LASNEX were input into XRASER to calculate the gains of the Ne-like laser lines, including radiation trapping effects on the 3s - 2p transitions and including bulk Doppler shifts. Our numerical results for the Asterix laser conditions show the $J=2-1$ emission peaking later in

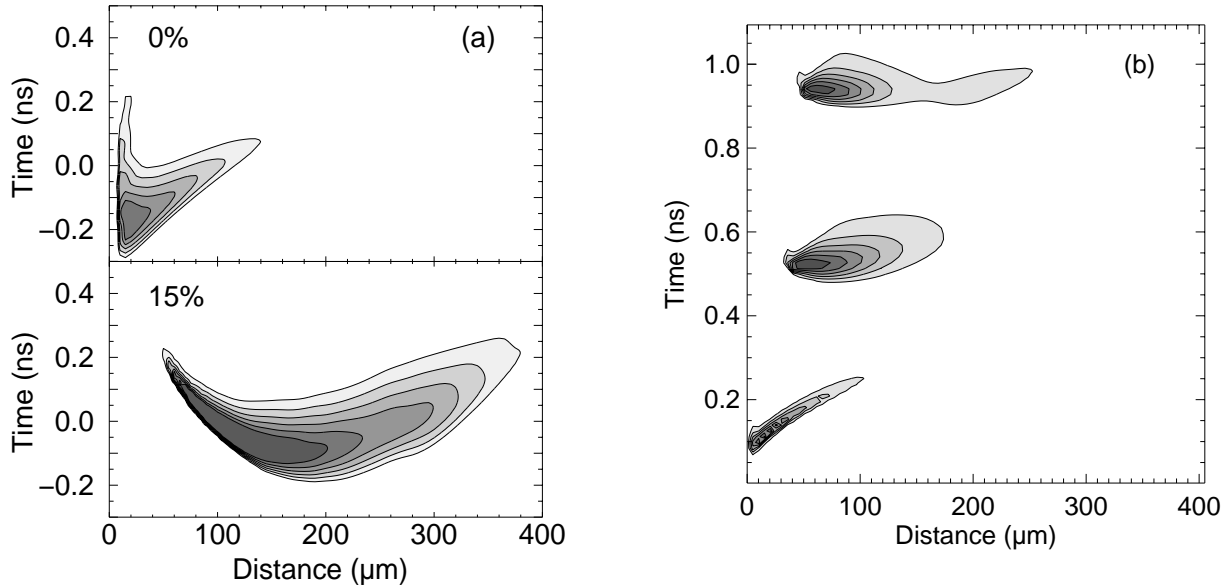


Figure 5. Contour plot of gain for Ne-like Ge $J=0-1$ line for three cases (a) no prepulse and 15% prepulse (b) three 100 ps pulses separated by 400 ps.

time and farther from the target surface than the $J=0-1$ emission, similar to other models¹¹⁻¹². The addition of a prepulse allows more plasma expansion and moves the peak emission region farther from the target surface in qualitative agreement with our observations. In the multiple pulse case, the gain region is very small and short lived during the first pulse. During the second and third pulses, which peak at 0.55 and 0.95 ns, the gain region becomes much larger and moves further from the target surface. The peak of the gain occurs 20-30 ps before the peak of the drive pulse about 50 to 60 μm from the surface. Our calculations also show that during the third pulse the gradients in the electron density become smaller while the density itself increases in the region of peak gain⁸.

The experiments, particularly the Nova experiments, show the laser emission peaking further from the target surface than the peak of the calculated gain. To understand this effect we performed a detailed calculation of the laser intensity (for the three pulse Nova experiments) at the output aperture including laser transport and refraction. We took the gain and density profiles at the time of peak gain for the second and third Nova pulses and did propagation calculations which amplified and refracted the beam down the 2.52 cm length of the plasma. We used the population of the upper laser state as a distributed source to mock up the amplified spontaneous emission nature of these lasers. Figure 6 shows the intensity versus distance

from the target surface from the refraction calculation along with a lineout of the experimental data averaged over the transverse dimension. While the experimental data is somewhat wider and has a longer tail, the agreement is nevertheless quite good. This shows that refraction of the laser has a large impact on the laser spatial distribution as well as the effective gain for a multiple pulse driven plasma. It is expected that refraction will play a somewhat smaller role in prepulse driven plasmas since the density gradients are smaller.

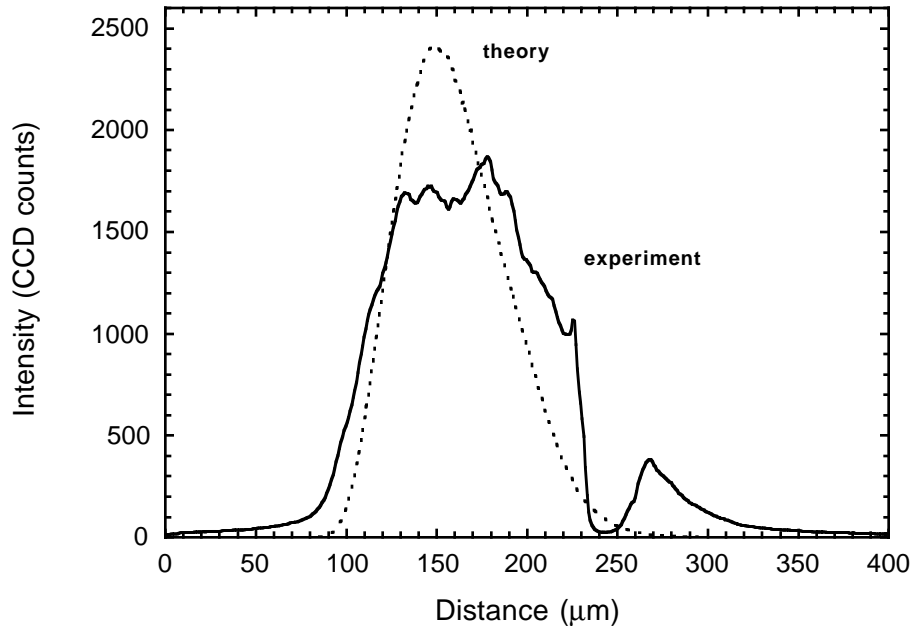


Figure 6. Spatial dependence of the calculated Ne-like Ge $J=0-1$ line intensity at 19.6nm (dotted line) at the output aperture of the laser. This is compared to the experimental data (solid line).

5. CONCLUSION

In summary we have obtained high resolution two-dimensional spatial images of the both the Ge $J=0-1$ and $J=2-1$ lines and the Ni $J=0-1$ line. For Ne-like Ge we have investigated both the prepulse and multiple pulse techniques. These images show the spatial extent and dependence of the Ge and Ni laser lines. For the prepulse case using the Asterix laser the $J=0-1$ line has more structure and peaks closer to the target surface than the $J=2-1$ lines. A larger prepulse shifts the peak outward from the target surface. The multiple pulse case also exhibits a great deal of structure both radially and transversely with the emission peaking at around 150 μm from the target surface. Simulations show the gain peaking only 50 - 60 μm from the surface, however our laser transport calculations, which include refraction effects, predict the peak emission 150 μm from the surface in good agreement with the experiments. Non-uniformities in both the drive laser and x-ray laser needs more investigation and may play a significant role in the development of a more coherent and efficient x-ray laser.

ACKNOWLEDGMENTS

The authors would like to thank S. Alvarez, H. Louis, J. Ticehurst and the Nova operations crew for providing support for these experiments. Y. Li and P. Lu were supported by the Alexander von Humboldt Foundation and Li was also partly supported within the framework of the agreement between the Max-Planck Society and the Academica Sinica. This work was supported in part by the Commission of the European Communities in the framework of the Association Euratom/Max-Planck-Institut für Plasmaphysik.

This work was performed under the auspices of the U. S. Department of Energy by the Lawrence Livermore National Laboratory under Contract No. W-7405-Eng-48.

REFERENCES

1. J. Nilsen, B. J. MacGowan, L. B. Da Silva, and J. C. Moreno, "Prepulse technique for producing low-Z Ne-like x-ray lasers," *Phys. Rev. A* **48**, pp. 4682-4685, 1993.
2. E. E. Fill, Y. Li, D. Schlogl, J. Steingruber, and J. Nilsen, "Sensitivity of lasing in neonlike zinc at 21.2 nm to the use of the prepulse technique," *Opt. Lett.* **20**, pp. 374-376, 1995.
3. Y. Li, G. Preztler, and E. E. Fill, "Ne-like x-ray lasers in the extreme ultraviolet region," *Phys. Rev. A* **52**, pp. 3433-3435, 1995.
4. Y. Li, G. Preztler, E. E. Fill, and J. Nilsen, "Temporally and spatially resolved investigation of the J=0-1 and J=2-1, 3p-3s lasers in neonlike germanium," *J. Opt. Soc. Am. B* **13**, pp. 742-750, 1996.
5. J. C. Moreno, J. Nilsen, and L. B. Da Silva, "Traveling wave excitation and amplification of neon-like germanium 3p-3s transitions," *Opt. Commun.* **110**, pp. 585-589, 1994.
6. H. Daido, R. Kodama, K. Murai, G. Yuan, M. Takagi, Y. Kato, I. W. Choi, and C. H. Nam, "Significant improvement in the efficiency and brightness of the J=0-1 19.6-nm line of the germanium laser by use of double-pulse pumping," *Opt. Lett.* **20**, pp. 61-563, 1995.
7. J. C. Moreno, J. Nilsen, Y. Li, P. Lu, and E. E. Fill, "Two-dimensional near-field images of the neonlike germanium soft-x-ray laser," *Opt. Lett.* **21**, pp. 585-589, 1996.
8. J. Nilsen, J. C. Moreno, L. B. Da Silva, and T. W. Barbee Jr., "Two-dimensional spatial imaging of the multiple-pulse-driven 196-Å neonlike germanium x-ray laser," *Phys Rev. A* **55**, pp. 827-830, 1997.
9. G. B. Zimmerman and W. L. Kruer, *Com. Plasma Phys. and Cont. Fusion* **2**, pp. 51 1975.
10. H. A. Scott and R. W. Mayle, "GLF - A simulation code for x-ray lasers," *Appl. Phys. B* **58**, pp. 35-43, 1994.
11. P. B. Holden and B. Rus, "A simple model of refraction in the Ne-like Zn, collisionally pumped laser," *Opt. Commun.* **119**, pp. 424-432, 1995.
12. J. A. Plowes, G. J. Pert, and P. B. Holden, "Double pulse irradiation of x-ray laser targets," *Opt. Commun.* **117**, pp. 189-197, 1995.

Technical Information Department • Lawrence Livermore National Laboratory
University of California • Livermore, California 94551